STRUCTURAL BIOLOGY COMMUNICATIONS

ISSN 2053-230X

Received 11 July 2019
Accepted 5 October 2019

Edited by R. L. Stanfield, The Scripps Research Institute, USA

‡ Present address: Illinois Mathematics and Science Academy, 1500 Sullivan Road, Aurora, IL 60506, USA.
§ Present address: SER-CAT and the Department of Biochemistry and Molecular Biology, University of Georgia, Athens, GA 30602, USA.

Keywords: high-affinity anti-cocaine antibody; antigen-binding fragment; crystal structure; benzoylecgonine complex; h2E2; Fab fragment.

PDB references: Fab fragment of anti-cocaine antibody h2E2, 6nex; bound to benzoyl-ecgonine, 6nfn

Supporting information: this article has supporting information at journals.iucr.org/f

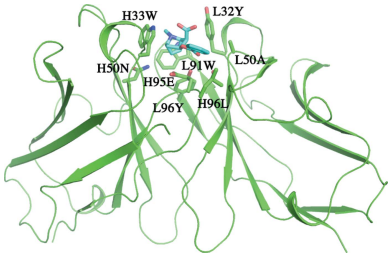

© 2019 International Union of Crystallography

Structural analysis of free and liganded forms of the Fab fragment of a high-affinity anti-cocaine antibody, h2E2

Kemin Tan,[a] Min Zhou,[b] Angela J. Ahrendt,[b]‡ Norma E. C. Duke,[b]§ Nassif Tabaja,[c] William J. Ball,[d] Terence L. Kirley,[d] Andrew B. Norman,[d] Andrzej Joachimiak,[a,e] Marianne Schiffer,[a] Rosemarie Wilton[b] and P. Raj Pokkuluri[a]*

[a]Structural Biology Center, X-ray Science Division, Argonne National Laboratory, Lemont, IL 60439, USA, [b]Biosciences Division, Argonne National Laboratory, Lemont, IL 60439, USA, [c]Department of Molecular Genetics, Biochemistry and Microbiology, University of Cincinnati, Cincinnati, OH 45267, USA, [d]Department of Pharmacology and Systems Physiology, College of Medicine and Microbiology, University of Cincinnati, Cincinnati, OH 45267, USA, and [e]Department of Biochemistry and Molecular Biology, University of Chicago, Chicago, IL 60637, USA. *Correspondence e-mail: ppokkuluri@gmail.com

A high-affinity anti-cocaine monoclonal antibody, designated h2E2, is entering phase 1 clinical trials for cocaine abuse therapy. To gain insight into the molecular details of its structure that are important for binding cocaine and cocaine metabolites, the Fab fragment was generated and crystallized with and without ligand. Structures of the unliganded Fab and the Fab fragment bound to benzoylecgonine were determined, and were compared with each other and with other crystallized anti-cocaine antibodies. The affinity of the h2E2 antibody for cocaine is 4 n*M*, while that of the cocaine metabolite benzoylecgonine is 20 n*M*. Both are higher than the reported affinity for cocaine of the two previously crystallized anti-cocaine antibodies. Consistent with cocaine fluorescent quenching binding studies for the h2E2 mAb, four aromatic residues in the CDR regions of the Fab (TyrL32, TyrL96, TrpL91 and TrpH33) were found to be involved in ligand binding. The aromatic side chains surround and trap the tropane moiety of the ligand in the complex structure, forming significant van der Waals interactions which may account for the higher affinity observed for the h2E2 antibody. A water molecule mediates hydrogen bonding between the antibody and the carbonyl group of the benzoyl ester. The affinity of binding to h2E2 of benzoylecgonine differs only by a factor of five compared with that of cocaine; therefore, it is suggested that h2E2 would bind cocaine in the same way as observed in the Fab–benzoylecgonine complex, with minor rearrangements of some hypervariable segments of the antibody.

1. Introduction

The ability of the mammalian adaptive immune system to generate high-affinity antibodies with specificities for virtually an unlimited number of antigens has long been exploited to develop a variety of therapeutic and diagnostic antibodies. Naturally occurring antigens generally consist of high-molecular-weight proteins, polypeptides, lipoproteins and lipopolysaccharides, while most low-molecular-weight biomolecules are not capable of generating an immune-system antibody response. However, low-molecular-weight molecules, such as commonly used drugs, can be manipulated into becoming immunogenic through linking them, as a hapten, to a larger immunogenic carrier protein in a manner that enables them to be recognized as active antigens by the immune system. Immunization protocols using hapten-carrier linked conjugates have enabled investigators to generate high-

affinity antibodies that are specifically directed against non-immunogenic compounds such as heroin, cocaine, nicotine and phencyclidine, the usage and abuse of which pose considerable individual as well as public health problems. These antibodies have the potential to be effective therapeutics in reducing abuse and relapse behaviors by sequestering the target drug in the plasma, thereby dramatically reducing drug distribution to the central nervous system and blunting neurological effects (Carrera *et al.*, 1995, 2000, 2001; Fox *et al.*, 1996; Kvello *et al.*, 2016; Cerny & Cerny, 2008; Kosten & Owens, 2005). Furthermore, the drug-binding Fab fragments or lower molecular weight scFv single-chain fragments derived from them, which have relatively fast elimination rates compared with intact antibodies, have the additional potential to be used as rescue treatment agents to assist detoxification in cases of acute overdoses of toxic drugs.

Human clinical trials using hapten-carrier vaccines that elicit endogenously produced polyclonal anti-nicotine and anti-cocaine antibodies have shown that a subset of vaccinated individuals can generate antidrug antibodies at levels sufficient to be therapeutically effective (Martell *et al.*, 2005, 2009). Alternatively, the use of murine hybridoma or phage-display methodologies, along with recombinant DNA technologies, has enabled the production of biomanufactured murine–human chimeric, humanized and human monoclonal antibodies (mAbs) that can be administered in known doses to provide immediate, high-affinity, passive immunization responses. As potential immunotherapeutics for the treatment of cocaine abuse, the murine-derived chimeric mAb GNC92H2 (Carrera *et al.*, 2005), the humanized mAb h2E2 (Norman *et al.*, 2014) and the fully human anti-cocaine mAb GNCgzk (Treweek & Janda, 2012) have been generated and characterized with regard to their affinities and specificities for cocaine and its metabolites. Additionally, in rodent models the *in vivo* ability of anti-cocaine mAbs to (i) decrease brain cocaine concentrations by restricting its distribution from plasma, (ii) increase the drug levels needed to reinstate cocaine-dependent self-administration behavior in trained rats and (iii) substantially reduce cocaine toxicity/lethality have been well documented (Treweek & Janda, 2012; Norman *et al.*, 2007, 2009; Norman & Ball, 2012; Wetzel *et al.*, 2016). Based on such preliminary studies, the mAb h2E2 is entering phase 1 clinical trials for cocaine abuse therapy.

In order to gain a better understanding of the molecular nature of anti-cocaine antibody–drug binding interactions, the Fab fragments of two anti-cocaine antibodies, the chimeric mAb GNC92H2 (IgG, $\gamma1, \kappa$) and the murine anti-cocaine mAb M82G2 (IgG, $\gamma1, \kappa$), have been crystallized and their detailed three-dimensional structures have been elucidated (Larsen *et al.*, 2001; Pozharski *et al.*, 2005). While these two mAbs and h2E2 all have selectivity for cocaine, some of the specifics of their binding characteristics are distinct. The GNC92H2 and h2E2 mAbs are similar in that they both bind cocaine and the active derivative cocaethylene with comparable affinities, with low affinity for inactive cocaine metabolites such as ecgonine methyl ester and ecgonine. However, the h2E2 mAb is unique in that it has a higher affinity for cocaine, with a K_d value of about $4 \times 10^{-9}\,M$ (Paula *et al.*, 2004), while GNC92H2 (Larsen *et al.*, 2001) and M82G2 (Pozharski *et al.*, 2005) have reported K_d values of 4×10^{-7} and $1.4 \times 10^{-7}\,M$, respectively, K_d values that are about 100-fold and 35-fold higher (lower affinity) than that of the h2E2 mAb utilized in the current study. Although both cocaine- and benzoylecgonine-bound Fab structures have been determined for the M82G2 mAb, its affinity for benzoylecgonine has not been reported. Antibody GNC92H2 has a 100-fold lower binding affiinity for benzoylecgonine than for cocaine (Larsen *et al.*, 2001).

The binding-affinity values in and of themselves provide no basic information about the mechanism and details of ligand interactions with the binding site of the antibody. Therefore, detailed structural information is required to begin to understand the interactions needed for the high-affinity, selective binding of cocaine. In the present work, we have determined the crystal structure of the Fab fragment of h2E2 both as a complex with benzoylecgonine (BE) and as a methylated form of the Fab fragment in the absence of bound ligand. In addition to presenting, analyzing and comparing the h2E2 Fab crystal structures, we compare the binding of benzoylecgonine by h2E2 with that in two previously determined Fab–ligand complex structures of other anti-cocaine antibodies. This broadens the perspective on what, if any, commonalities exist with regard to how mAbs bind cocaine, as well as the limitations that may exist for generating mAbs with high-affinity and selective binding sites for low-molecular-weight antigens.

2. Materials and methods

2.1. Materials

Endoproteinase Lys-C (lysyl endoproteinase, *Achromobacter* protease I, Endo-Lys-C; catalog No. 129-02541) was obtained from Wako Pure Chemicals. HEPES buffer was from Sigma (catalog No. H-3375). NaCl was from Fisher Scientific. Borane–dimethyl complex (97%) was obtained from Sigma–Aldrich (catalog No. 180238) and 37% formaldehyde was from Sigma (catalog No. F8775). Concentrated formic acid, sequencing grade, was purchased from Fisher Scientific. Cocaine hydrochloride (catalog No. C-5776) was obtained from Sigma–Aldrich. GeneArt Seamless Cloning reagents (Invitrogen) were from Thermo Fisher Scientific. KOD polymerase (EMD Millipore, Billerica, Massachusetts, USA) was used for PCR amplification. Plasmid miniprep and PCR purification kits were from Qiagen (Germantown, Maryland, USA). Synthetic DNA and oligonucleotides were obtained from Integrated DNA Technologies (IDT; Coralville, Iowa, USA) and Blue Heron Biotech (Bothell, Washington, USA). Unless otherwise indicated, all other chemicals and reagents were from Sigma (St Louis, Missouri, USA) or Thermo Fisher Scientific (Waltham, Massachusetts, USA).

2.2. Expression from *Escherichia coli* and purification of recombinant h2E2 Fab

2.2.1. Vector construction. Amino-acid sequences for the h2E2 heavy-chain and light-chain variable domains as well

as for the human lambda 2 constant domain were reverse-transcribed and optimized for expression in *E. coli* using the Blue Heron Biotech online codon-optimization tool (https://www.blueheronbio.com/codon-optimization). Synthetic DNA for the heavy- and light-chain variable domains was obtained from Blue Heron Biotech, and the lambda 2 constant domain was obtained as a gBlock from IDT. Coding regions for the h2E2 Fab were introduced into the plasmid pASK88-D1.3 (a kind gift from Arne Skerra, Technische Universität München, Germany) by stepwise replacement of the analogous regions of the D1.3 anti-lysozyme Fab using GeneArt Seamless Cloning. Firstly, the vector was PCR-amplified with primers that eliminated the light-chain constant domain, and the PCR product was then treated with DpnI to remove the plasmid template. The gBlock fragment coding for the human lambda 2 constant domain, which contained 16 bp vector overlaps, was assembled with the PCR-amplified vector using the GeneArt Seamless Cloning and Assembly Enzyme Mix (Invitrogen). The resulting vector was then amplified for assembly with the PCR-amplified V_H coding region, and finally the process was repeated a third time to insert the V_L domain. The pAKS88-D1.3 vector contained a human IgG1 C_H1 domain that was identical to that of the h2E2 monoclonal antibody except for a ^{210}Arg to Lys change near the C-terminal end of C_H1. This domain was retained in the final h2E2 recombinant Fab expression vector. Cloned inserts were verified by Sanger sequence analysis (University of Chicago Comprehensive Cancer Center DNA Sequencing and Genotyping Facility, Chicago, Illinois, USA). The sequences of the PCR primers, sequencing primers and synthetic DNA are provided in Supplementary Tables S1–S4.

2.2.2. Expression and purification of recombinant h2E2 Fab (rFab). *E. coli* strain JM83 (Yanisch-Perron *et al.*, 1985) harboring pASK88-h2E2 and the helper plasmid pTum4 (Schlapschy *et al.*, 2006; a kind gift from Arne Skerra, Technische Universität München, Germany) was grown in shake flasks at 37°C using M9 medium supplemented with glycerol, glucose, amino acids, trace metals and vitamins (Donnelly *et al.*, 2006). Ampicillin (100 µg l^{-1}) and chloramphenicol (30 µg l^{-1}) were added to maintain the plasmids. At mid-log phase, the culture temperature was reduced to 25°C. Expression was then induced with anhydrotetracycline, which was added to a final concentration of 0.2 mg l^{-1}. After overnight growth, the cells were harvested by centrifugation in 1 l centrifuge bottles. Each pellet was resuspended in 25 ml TES buffer (0.2 *M* Tris–HCl, 0.5 m*M* EDTA, 0.5 *M* sucrose pH 8.0) plus one cOmplete protease-inhibitor tablet (Roche) by shaking at 200 rev min^{-1} at 4°C. After the pellets had been completely resuspended, 50 µl of 100 mg ml^{-1} lysozyme and 25 ml ice-cold water were added and the suspension was incubated at 4°C for 1 h with agitation at 70 rev min^{-1}. Spheroplasts were removed by centrifugation for 30 min at 30 000*g* and the supernatant constituted the periplasmic fraction. The rFab was purified from the periplasmic fraction by nickel-affinity chromatography on an ÄKTAexplorer 3D using an established protocol (Kim *et al.*, 2004). The eluted protein was further purified by size-exclusion chromatography on a Superdex 200 (26/60) column in 20 m*M* HEPES, 100 m*M* NaCl pH 8.0. Fractions containing purified rFab were identified by SDS–PAGE under reducing conditions and were combined and concentrated to 18 mg ml^{-1} using a centrifugal filter unit. A culture volume of 8 l yielded approximately 3 mg recombinant h2E2 Fab (rFab).

2.3. Preparation and characterization of the Fab from the h2E2 mAb and reductive methylation of the Fab fragment

The Fab fragment of the h2E2 anti-cocaine mAb was generated by Endo-Lys-C digestion followed by purification, as described previously (Kirley & Norman, 2015). The Fab fragment was reductively methylated on lysine residues as a way to aid crystallization, basically as described previously (Walter *et al.*, 2006; Tan *et al.*, 2014). For more details, see the supplementary information.

To ensure that methylation did not negatively affect the binding of cocaine to the Fab fragment, the methylated Fab fragment was examined for cocaine binding using the fluorescence assay reported previously (Kirley & Norman, 2015). Cocaine binding to the Fab and mFab was measured by monitoring the change in intrinsic protein tyrosine and tryptophan fluorescence upon titration with ligand at 20°C. Briefly, measurements of intrinsic protein fluorescence and quenching of that fluorescence by cocaine were made using a Hitachi F-2000 fluorescence spectrophotometer. 2 ml Fab solutions in Tris-buffered saline (TBS) were analyzed and titrated with ligands, measuring the emission at 330 nm with excitation at both 280 and 295 nm after each addition of ligand.

The K_d for cocaine of the methyl-Fab was measured to be 1.2 $\pm$ 0.3 n*M* (using tryptophan-selective excitation at 295 nm). This value is actually slightly less (a slightly higher affinity) than we reported for the unmodified Fab fragment using the same methodology (3.8 $\pm$ 1.6 n*M*; Kirley & Norman, 2015).

2.4. Crystallization and diffraction data collection

2.4.1. Fab–benzoylecgonine complex. The purified and concentrated rFab (18 mg ml^{-1}) was mixed with cocaine hydrochloride (to a final cocaine concentration of 10 m*M*) and the mixture was incubated on ice for 2h. The Fab/cocaine mixture was then screened for crystallization conditions with a Mosquito liquid dispenser (TTP Labtech, Cambridge, Massachusetts, USA) using the sitting-drop vapor-diffusion technique in 96-well CrystalQuick plates (Greiner Bio-One, Monroe, North Carolina, USA). Several commercially available crystallization screens were used. For each condition, 0.4 µl Fab/cocaine solution and 0.4 µl crystallization formulation were mixed and the mixture was equilibrated against 135 µl crystallization formulation in the well at 16°C. Diffraction-quality crystals appeared after two months under a condition consisting of 2% Tacsimate pH 7, 0.1 *M* HEPES pH 7.5, 20% PEG 3350 (condition G10 of PEG/Ion HT from Hampton Research, Aliso Viejo, California, USA). Before data collection, the crystals were treated with a cryoprotectant composed of the crystallization reagent plus 25%(*v*/*v*)

Table 1
Crystallographic and data-collection parameters.

Values in parentheses are for the highest resolution shell.

	rFab–BE complex	Free mFab
Unit-cell parameters (Å, °)	a = 70.05, b = 85.84, c = 164.4, α = 82.9, β = 81.8, γ = 71.3	a = 110.8, b = 128.4, c = 91.20, β = 125.3
Space group	$P1$	$C2$
No. of molecules in asymmetric unit	8	2
V_M (Å^3 Da^{-1})	2.5	2.9
Solvent content (%)	51	57
Wavelength (Å)	0.97915	0.97919
Resolution (Å)	38.6–2.63 (2.68–2.63)	27.8–2.15 (2.19–2.15)
No. of unique reflections	104134	54989
R_{merge}	0.119 (0.805)	0.054 (0.869)
R_{meas}	0.140 (0.970)	0.062 (1.009)
$R_{p.i.m.}$	0.075 (0.537)	0.030 (0.506)
$CC_{1/2}$	0.983 (0.572)	0.998 (0.639)
Multiplicity	3.5 (3.1)	4.1 (3.7)
Completeness (%)	98.3 (98.5)	97.9 (96.2)
Mean $I/\sigma(I)$	13.9 (1.6)	32.7 (2.3)
Wilson B factor (Å^2)	45.7	44.7

Table 2
Refinement statistics.

	rFab–BE complex	Free mFab
Program used	*Phenix*	*Phenix*
Resolution range (Å)	38.60–2.63	27.8–2.15
No. of reflections	104051	54930
R factor	0.185	0.214
R_{free}†	0.244	0.254
No. of non-H atoms		
Protein	24869	6169
Heteroatoms	220	206
Waters	173	111
Mean B factor (Å^2)		
Protein	61.7	74.1
Heteroatoms	51.5	71.0
Waters	47.4	55.5
R.m.s.d.s		
Bonds (Å)	0.004	0.003
Bond angles (°)	0.72	0.60
Ramachandran plot (%)		
Favored regions	95.3	95.6
Outliers	0.4	0
PDB code	6nfn	6nex

† The test set consisted of 5% of the reflections.

glycerol. X-ray diffraction data were collected at 100 K on the 19ID beamline of the Structural Biology Center at the Advanced Photon Source (APS), Argonne National Laboratory using *SBCcollect* (Rosenbaum *et al.*, 2006). The best data set was processed to 2.63 Å with the *HKL*-3000 suite (Minor *et al.*, 2006; Table 1).

2.4.2. Unliganded (free) Fab. Purified and concentrated methyl-Fab (mFab; 10 mg ml^{-1}) was screened at 16°C using the commercial crystallization screens MCSG-1, MCSG-2, MCSG-3 and MCSG-4 (Microlytic Inc.). The crystallization drops were set up using a Mosquito liquid dispenser as described above. An initial hit was observed in condition A7 from MCSG-2. Further optimization was carried out manually using the hanging-drop vapor-diffusion method by setting up crystallization drops at room temperature consisting of 1 µl protein solution and 1 µl well solution using Linbro plates equilibrated against a volume of 0.5 ml. Crystals usually appeared within a day and grew to full size in a week. The crystal used for data collection was obtained from Wizard II condition No. 36 diluted with water (8% PEG 3000, 80 m*M* phosphate–citrate pH 4.2, 160 m*M* NaCl). The crystals were unstable (breaking apart and dissolving rapidly) when transferred to cryoprotectant solution consisting of the reservoir solution supplemented with 25% glycerol or ethylene glycol. Therefore, a crystal from the mother liquor was directly transferred to liquid nitrogen. *In situ* annealing of the crystal for 10 s alleviated the initially observed problem of ice rings. Data collection was carried out on the 19BM beamline at APS. The crystallographic parameters are included in Table 1 and the refinement statistics are given in Table 2.

2.5. Structure determination and refinement

2.5.1. Fab–benzoylecgonine complex. The rFab–benzoylecgonine complex crystals belonged to space group $P1$. The data could not be scaled in a higher symmetry space group. The structure of the complex was solved by the molecular-replacement method using *MOLREP* (Vagin & Teplyakov, 2010) within the *HKL*-3000 suite (Minor *et al.*, 2006). The V_LV_H pair of the Fab from the hH35 antibody Fab–human hepsin complex structure (Koschubs *et al.*, 2012; PDB entry 3t2n) was first used as a search template. The search resulted in the location of eight V_LV_H pairs in one asymmetric unit of the crystal with a correlation coefficient of 35.3%. After several cycles of rigid-body and position/displacement refinements, the above model containing eight V_LV_H pairs were fixed while the C_LC_{H1} pair from the same Fab (PDB entry 3t2n) was used as a search template, resulting in the locations of all eight C_LC_{H1} pairs in the asymmetric unit with a correlation coefficient of 53.6%. After several cycles of refinement, automatic model rebuilding with *Buccaneer* (Cowtan, 2008) within the *HKL*-3000 package was performed, which led to the building of a model with correlation coefficients of 92% for the main chain and 79% for the side chains of all eight Fabs. The completion of the structural model, including the addition of ligand molecules, was performed manually using *Coot* (Emsley *et al.*, 2010). The final refinement cycles were performed with *Phenix* (Adams *et al.*, 2010). The structure solution by molecular replacement placed two clusters of four Fabs each. Within each cluster of four Fabs there is an approximate fourfold symmetry between them.

2.5.2. Unliganded Fab. The structure was determined by molecular replacement using *Phaser* (McCoy *et al.*, 2007). The Fab portion of the h2E2 rFab–benzoylecgonine complex structure (this work) was used as the search structure. The final structure was refined by *Phenix* to a resolution of 2.15 Å with an R factor and R_{free} of 0.214 and 0.254, respectively. The crystallographic parameters are included in Table 1, whereas the refinement statistics are shown in Table 2. In the case of the unliganded mFab crystals the two Fabs per asymmetric unit are related by pseudo-twofold symmetry but were refined independently.

A schematic view of the interactions of benzoylecgonine and h2E2 Fab was generated by *LigPlot+* (Laskowski & Swindells, 2011). All other structural figures were generated with *PyMOL* (http://pymol.org). Elbow-angle calculations were performed using the web server at http://proteinmodel.org/AS2TS/RBOW/index.html (Stanfield *et al.*, 2006).

3. Results

3.1. Expression of recombinant h2E2 Fab in *E. coli*

Recombinant h2E2 Fab (termed rFab) was produced with the *E. coli* expression vector pASK88 (Schiweck & Skerra, 1995). In this vector, the two polypeptides of the Fab are expressed as an operon under the tightly regulated control of the *tetA* promoter, and secretion of the heavy- and light-chain components is directed to the periplasm for proper folding and assembly via the OmpA and PhoA signal peptides (Skerra, 1994*a*,*b*). A His_6 affinity tag is appended to the C-terminal end of the heavy chain to simplify purification. The h2E2 expression cassette was constructed using *E. coli* codon- and expression-optimized synthetic DNA. Fragments coding for the 2E2 V_H, V_L and human lambda 2 constant domains were assembled in pASK88 using seamless cloning techniques. pASK88 carries a human IgG1 heavy-chain constant domain 1 ($C_H1_{\gamma1}$), which is identical to that in the h2E2 antibody except for the presence of Lys at position 210 (h2E2 has Arg at this position). For the purpose of this study, this residue was not changed as it was not expected to affect the structure or function of the binding site of the antibody. h2E2 rFab was expressed in shake flasks with an *E. coli* strain carrying the helper plasmid pTUM4 to facilitate the proper folding and assembly of the polypeptides in the periplasm (Schlapschy *et al.*, 2006). After purification, the yield ranged from 0.3 to 0.4 mg rFab per litre of shake-flask culture.

3.2. Crystallization and structure determination of rFab in the presence of cocaine

Crystallization trials were carried out with the rFab alone and in the presence of cocaine. After two months, diffraction-quality crystals were produced in one condition (2% Tacsimate pH 7, 0.1 *M* HEPES pH 7.5, 20% PEG 3350) in a drop containing rFab and cocaine. The rFab complex crystals belonged to space group *P*1, with unit-cell parameters $a = 70.05$, $b = 85.84$, $c = 164.4$ Å, $\alpha = 82.9$, $\beta = 81.8$, $\gamma = 71.3^\circ$. The structure was determined by the molecular-replacement method as outlined in Section 2 and was refined to 2.63 Å resolution, with a final R factor of 0.185 and R_{free} of 0.244. Table 1 lists the data-collection parameters and Table 2 shows the refinement parameters. The crystals contained eight copies of the rFab complex per asymmetric unit.

Although the Fab complex crystals were obtained from a drop containing Fab and cocaine, the structure revealed that the hapten observed bound to the Fab in the crystals was BE and not cocaine. In all eight copies of the complex that were refined independently in the crystal, the electron-density map shows a carboxyl group at the C2 position of the tropane ring system but not a methyl ester, consistent with BE and not cocaine. In five of the copies of the Fab complex molecule in the crystal, the electron density supported the modeling of a water molecule near the carboxyl group of benzoylecgonine.

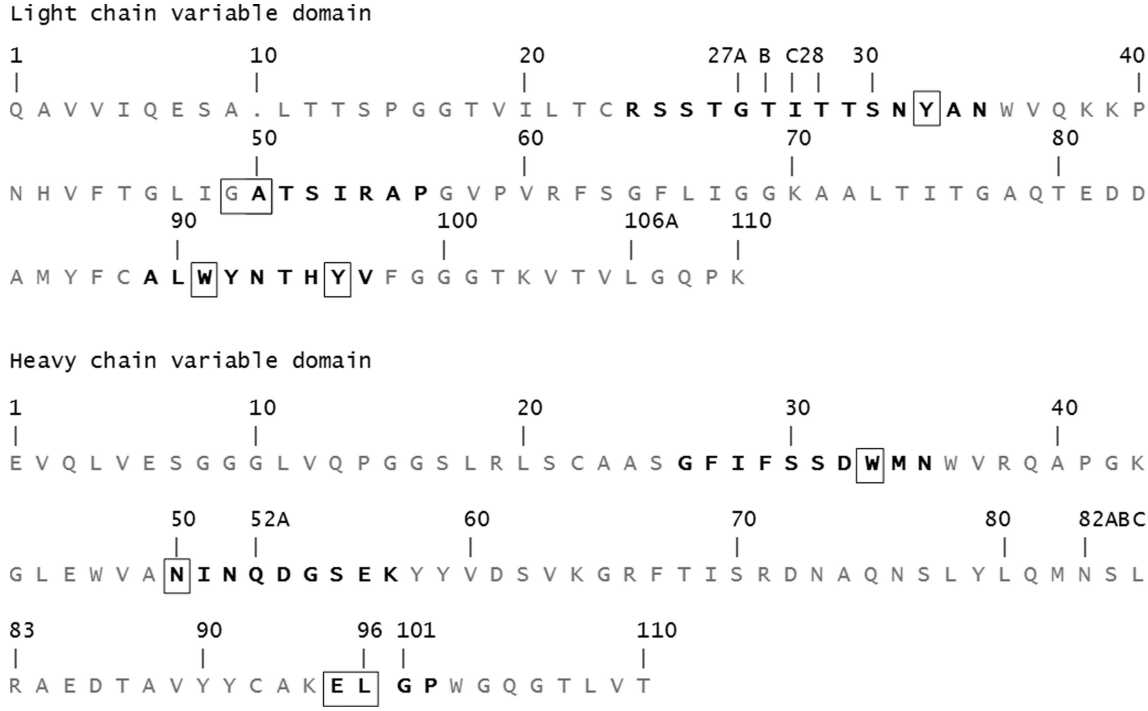

Figure 1
The amino-acid sequence of the variable domains of h2E2 Fab. The Kabat numbering for the variable-domain residues is shown. The CDRs are indicated in bold. Residues with contacts within 4.0 Å of the ligand are boxed.

Non-enzymatic hydrolysis of the methyl ester group of cocaine is efficient at ambient temperature and at pH values above 5.5 (Das Gupta, 1982; Warner & Norman, 2000; Murray & Al-Shora, 1978). Although the above-reported conditions are not the same as those used in our crystallization trials, the complex crystals were observed after two months at 16°C employing neutral pH conditions (pH 7.5). The hydrolysis of the methyl ester group of cocaine resulted in the formation of BE, which subsequently complexed with the Fab and produced crystals. No crystals were observed early in the experiment when the cocaine would have been intact.

3.3. Overall structure of the h2E2 Fab–benzoylecgonine complex

The amino-acid sequence of the variable domains of h2E2 Fab is shown in Fig. 1. The structure of the h2E2 Fab shows the typical immunoglobulin light (L) and heavy (H) chains organized with the two variable domains, V_H and V_L, related by a pseudo-twofold axis and the two constant domains, C_{H1} and C_L, related by another pseudo-twofold axis. The BE binding site is provided by the three complementarity-determining regions (CDRs) of V_H and V_L domains, termed H1, H2, H3 and L1, L2, L3 (see Fig. 1 for the sequence; Kabat numbering is shown). There are eight copies of the Fab–BE complex in the asymmetric unit of the crystal, which were independently refined without any noncrystallographic symmetry imposed on them. The electron density is of good quality except for one segment connecting the β-strands in the

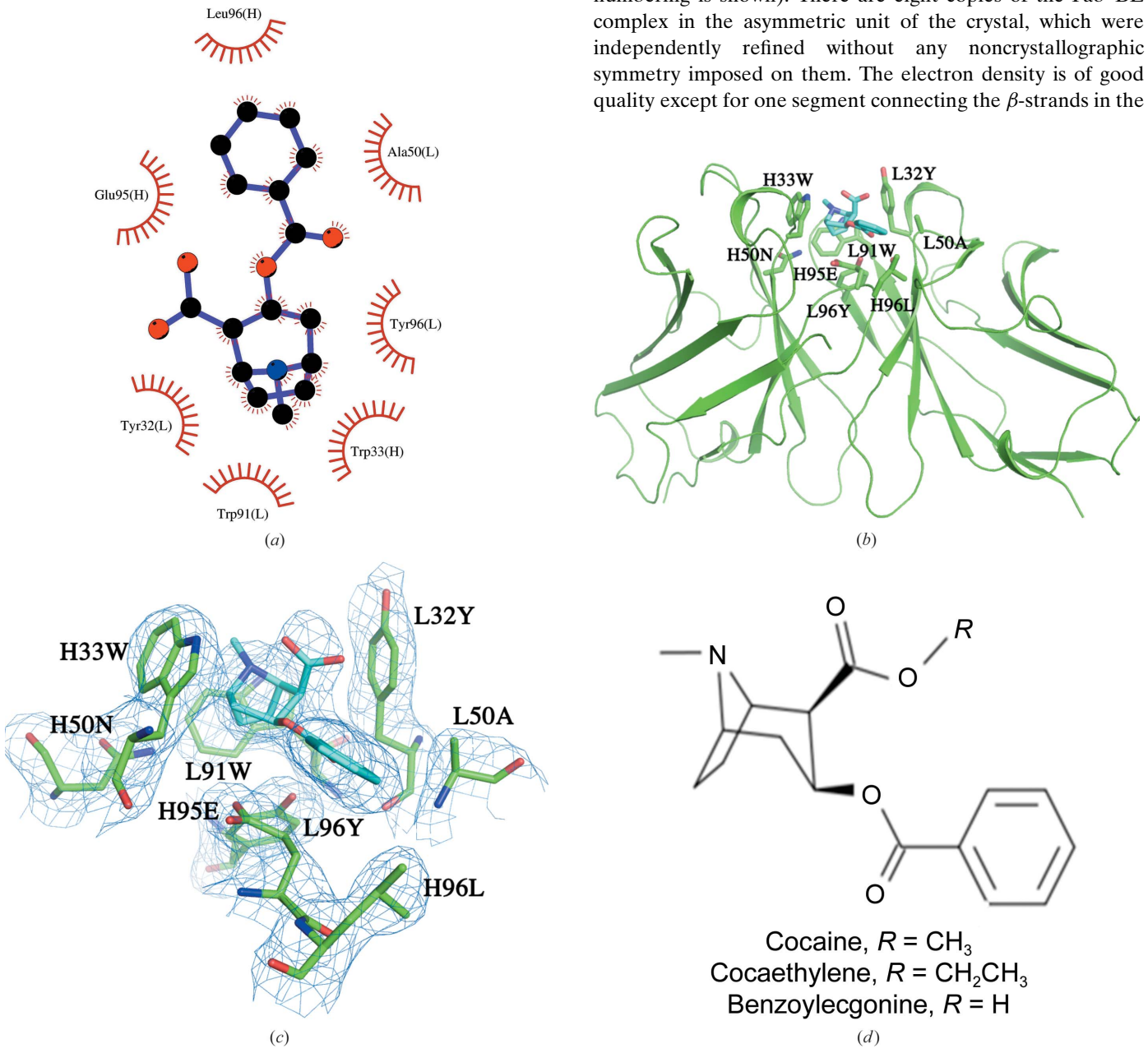

Figure 2
(*a*) A schematic view of the interactions of benzoylecgonine and h2E2 Fab generated by *LigPlot+* (Laskowski & Swindells, 2011). (*b*) A view of the complex structure showing the binding-site interactions between benzoylecgonine (C atoms in cyan) and the variable-region residues of the h2E2 Fab (C atoms in green). The ligand and the binding residues from the Fab are shown as stick drawings, whereas the V_L and V_H domains are shown as a C^{α} carton in green. (*c*) A view of the electron density observed in a $2mF_o - DF_c$ OMIT map is shown for benzoylecgonine and the surrounding residues contoured at 1σ. (*d*) Chemical representation of cocaine and its analogs benzoylecgonine and cocaethylene.

constant domain of the heavy chain, residues 127–135, that was not modeled. The electron density at the C-terminal end of the H chain was also of poor quality in some of the Fab molecules in the asymmetric unit. The H-chain electron density was visible to Pro213, and the rest of the chain, including the His_6 tag at the C-terminus, was presumed to be disordered since there was no discernable electron density in the maps corresponding to this sequence. The light-chain electron density was visible to Pro211, with the last four C-terminal residues absent from the electron-density maps.

3.4. Fab–benzoylecgonine interactions

The benzoylecgonine moiety was observed to bind in a shallow groove formed by the CDR loops of the Fab, which contain an impressive array of aromatic side chains, as shown in Fig. 2. Benzoylecgonine was bound to the CDR loops of the Fab entirely through van der Waals interactions, without any direct hydrogen bonds or charge–charge interactions. The interactions between benzoylecgonine and the Fv are the same in all eight Fabs in the complex crystals, suggesting that the binding site is rigid and was not affected by the crystal packing. The residues contacting BE from the Fab include light-chain CDR loops L1 (Tyr32), L2 (Ala50) and L3 (Trp91 and Tyr96) and heavy-chain CDR loops H1 (Trp33), H2 (Asn50) and H3 (Glu95 and Leu96), resulting in a total of 65 contacts within a 4.0 Å cutoff distance. Although GlyL49 is not considered to be part of CDR L1, it does contact the ligand. The BE tropane ring system is surrounded by aromatic side chains of TyrL32, TrpL91, TyrL96 and TrpH33. One cation–π interaction can be described for TrpH33, for which the center of the aromatic ring is at a distance of 4.0 Å from the positively charged N atom of the tropane ring. Interestingly, the benzoyl ring of BE makes no contacts with the aromatic side chains of the Fab; instead, the contacts were provided by GlyL49, AlaL50, GluH95 and LeuH96.

The carboxylic acid group of BE is fully exposed to the solvent with no contacts with the Fab within 4 Å (see Figs. 2*b* and 3). A water molecule mediates hydrogen-bond interactions between the carbonyl group of the BE benzoyl ester and the main-chain O atom of TyrL32 and between the main-chain N atom of AlaL50 and the side-chain hydroxyl group of TyrL96.

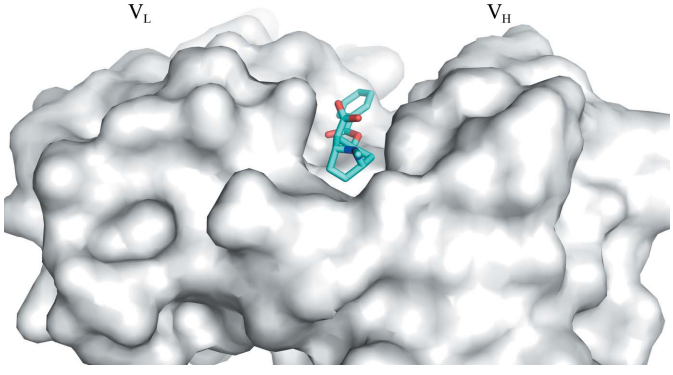

Figure 3
A surface (gray) rendering of h2E2 Fab showing the binding site of benzoylecgonine (stick drawing) located in a surface groove.

3.5. Structure of the unliganded (or free) Fab

Crystallization trials carried out with the purified, unliganded Fab fragment produced by proteolysis of the h2E2 antibody resulted in poor-quality crystals under many conditions containing PEG as a precipitant. Extensive attempts to optimize these conditions did not prove successful. Subsequently, the purified Fab fragment was subjected to reductive methylation of lysines as described in Section 2. The resulting Fab sample is termed mFab. This facilitated the crystallization of the Fab fragment. Importantly, lysine methylation of the Fab did not diminish its affinity for cocaine. The unliganded mFab crystals belonged to space group *C*2, with unit-cell parameters a = 110.8, b = 128.4, c = 91.2 Å, β = 125.3°. The structure was determined by molecular replacement using the Fab portion of the structure of the benzoylecgonine complex.

3.6. Structural comparison of the free Fab and the complex

A structural overlap of the variable domains of unliganded mFab and the rFab–BE complex is shown in Fig. 4. Since the free and complex Fabs crystallized in different unit cells and space groups, comparison between them is complicated by the effects of crystal packing on local conformations and different elbow angles. Caution should be taken in the interpretation of the changes that are observed. Comparison of the Fv (both V_L and V_H) of one free Fab (chains *L* and *H*) with one of the complexed Fabs (chains *A* and *B*) with the closest elbow angle resulted in an r.m.s.d. of 0.6 Å, whereas the same comparison with the other Fab molecule found in the free Fab crystal shows an r.m.s.d. of 0.7 Å. When the individual variable

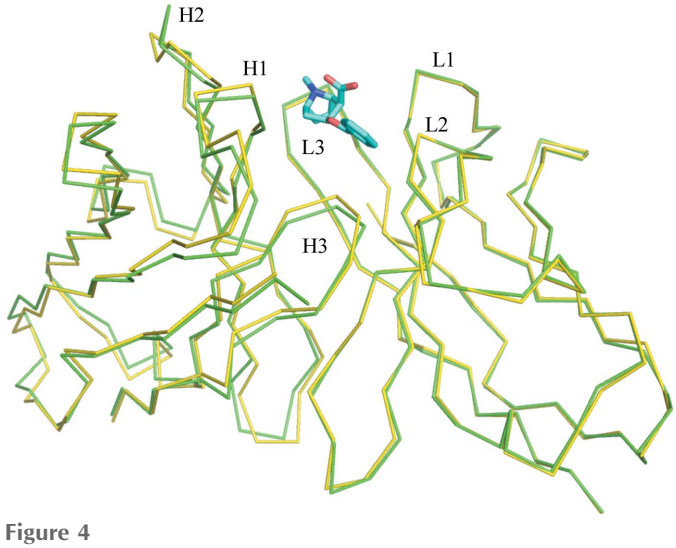

Figure 4
A view of the C^{α} trace of the structural overlap of unliganded and liganded h2E2 Fab. The light-chain V domains are superposed to illustrate the deviations in the heavy-chain variable domain. Complex/liganded Fab is in green and free/unliganded Fab is in yellow. The ligand is shown as a stick drawing (C atoms in cyan, O atoms in red, N atoms in blue). The V_H domain is on the left and the V_L domain is on the right. The CDR loops are labeled.

domains are compared (*i.e.* V_L versus V_L and V_H versus V_H), the r.m.s.d.s are 0.3 and 0.7 for the V_L domains and 0.4 and 0.6 for the V_H domains, respectively, for the two Fabs found in the free Fab crystals. The CDR loops did not show any larger deviations compared with other parts of the variable domains. Fig. 4 highlights the deviations observed in the respective V_H domains when the two V_L domains are superimposed, reflecting a minor variation in the V_L/V_H association between the free Fab and the complexed Fab. The elbow angles observed for the Fab molecules in the crystals of both the complex and the unliganded structures are presented in Supplementary Table S5.

4. Discussion

As mentioned in Section 1, two structures of antibody Fab–cocaine complexes have previously been published for the anti-cocaine antibodies M82G2 and GNC92H2. The antibody GNC92H2 was generated using benzoylecgonine conjugated to keyhole limpet hemocyanin (KLH) via a six-carbon adipic acid linker at the C2 ester site as an antigen. The mAb 2E2, like GNC92H2, was raised to benzoylecgonine (BE) coupled to KLH but linked via an amide bond rather than an ester, using 1,4-diaminobutane as a linker (see Supplementary Fig. S1). The difference between 2E2 and h2E2 is that in the humanized version the constant domain of the mouse lambda light chain is replaced by the human light-chain constant domain. The M82G2 antibody was also raised against a BE hapten but linked at the *p*-benzoyl position via a short thiocyanate coupler to bovine testes β-galactosidase. In addition, the structure of the cocaine-degrading catalytic antibody 7A1 Fab has been reported in complex with cocaine (Zhu *et al.*, 2006). The structure of the 7A1 Fab–cocaine complex (PDB entry 2ajv) shows that cocaine is bound on a surface groove similar to the h2E2 complex, but the dissociation constant for cocaine binding for this antibody was not reported.

4.1. Crystallization

It is important to note the differences in the two h2E2 Fab samples (rFab versus mFab) used in the present study, which probably affected their crystallization behavior. The two protein samples differ at the C-terminal end of the heavy chain. The C-terminal amino-acid sequence of the heavy chain of the Fab obtained by proteolytic cleavage of the IgG is ^{210}RVEPKSCDK^{218}, whereas the sequence of the heavy chain in the *E. coli*-produced rFab is ^{210}KVEPKSCHHHHHH^{222}. The former sample modified further by reductive methylation of lysines (mFab) was used in the production of apo Fab crystals, whereas the latter sample was used for the Fab–BE complex.

Although reductive methylation of the h2E2 Fab produced by cleavage of the mAb allowed the identification of conditions for crystallization of the unliganded protein, no crystals were produced in the presence of cocaine under the same crystallization conditions. This implies that the Fab structure bound to cocaine (or benzoylecgonine) is not compatible with the packing of molecules in this crystal form. Indeed, in the apo crystals the ligand-binding site is involved in crystal contacts in one of the two Fab molecules in the asymmetric unit. The side chains of the ligand-binding residues Tyr34 and Trp93 of the light chain form hydrogen bonds to the main-chain atoms of a crystallographically related molecule (see Supplementary Table S6 for details). In addition, the aromatic side chain of Trp93 forms cation–π interaction with a lysine residue across the crystallographic interface. Not surprisingly, attempts to soak cocaine into apo Fab crystals were not successful. Transfer of the apo crystals to mother liquor containing cocaine resulted in the immediate breakup and dissolution of the crystals. Future experiments will involve the identification of a new crystal form of the apo Fab in which the binding site is not occluded and a search for conditions for h2E2 Fab–cocaine complex crystallization at low pH ($\leq$5) that inhibit the hydrolysis of cocaine.

4.2. Hapten recognition by h2E2

As predicted by the previous computational docking modeling study of cocaine binding by the 2E2 Fab (Lape *et al.*, 2010), benzoylecgonine binds not in a pocket but in a groove situated between the V_H and V_L domains. The recognition of the benzoylecgonine ligand by the h2E2 Fab is primarily driven by aromatic side chains trapping the tropane ring system. This is consistent with the large quenching of h2E2 mAb tyrosine and tryptophan fluorescence, which was used to measure the binding of cocaine and BE to intact h2E2 as well as to the h2E2 Fab fragment (Kirley & Norman, 2015). In the conformation of benzoylecgonine observed in the h2E2 Fab complex structure, the methyl group of the ester which would be present in cocaine or the ethylene group which would be present in cocaethylene would be fully exposed to solvent and would not contact the Fab (see Figs. 2*b* and 3). The BE-binding residues or the crystal contacts observed in the present Fab complex structure do not preclude the possibility of cocaine binding to the Fab in exactly the same orientation. No steric conflicts were observed when benzoylecgonine in the binding site is replaced by cocaine *in silico* (see the surface rendition of the binding site in Fig. 3, which shows the carboxyl group exposed to solvent) in any of the eight independent Fab molecules. However, the origin of the observed selectivity of h2E2 for cocaine and cocaethylene relative to benzoylecgonine (K_d of 1 n*M* for cocaethylene and 4 n*M* for cocaine compared with 20 n*M* for benzoylecgonine) is not apparent from this structure (Kirley & Norman, 2015). Cocaine/cocaethylene binding could be accompanied by minor changes in the conformation of the h2E2 CDR loops. It is unlikely that cocaine and cocaethylene have a completely different binding orientation compared with benzoylecgonine, especially considering the relatively small differences in the binding energies deduced from the abovementioned K_d values (a 0.8 kcal mol^{-1} gain in free energy in the case of cocaine compared with BE and a 1.8 kcal mol^{-1} gain in free energy in the case of cocaethylene compared with BE).

Table 3
Comparison of the number of van der Waals contacts and hydrogen bonds (the distance cutoff between non-H atoms is ≤3.2 Å) between the ligand (cocaine or benzoylecgonine) and the Fab in various complex structures.

The numbers of water molecules mediating hydrogen bonds between the ligand and the Fab are included in a separate column.

Fab complex	No. of contacts (≤4.0 Å)	No. of hydrogen bonds	No. of water molecules mediating hydrogen bonds
h2E2 (benzoylecgonine; this study)	66	0	1
PDB entry 1qyg (benzoylecgonine; Pozharski *et al.*, 2005)	103	2	2
PDB entry 1q72 (cocaine; Pozharski *et al.*, 2005)	93	0	1
PDB entry 1i7z (cocaine; Larsen *et al.*, 2001)	68	0	1

4.3. Comparison of the h2E2 Fab complex with the Fab complexes of the M82G2 and GNC92H2 anti-cocaine antibodies

The antibodies M82G2 (Pozharski *et al.*, 2005) and GNC92H2 (Larsen *et al.*, 2001) bind cocaine with a much lower affinity (micromolar dissociation constants) compared with h2E2 (nanomolar dissociation constant). All three antibodies consist of IgG1 heavy chains, but the previously reported antibodies both have a kappa light chain, while h2E2 contains the less common lambda light chain and therefore has a V_L domain sequence that is quite distinct from the kappa light chains of the other two anti-cocaine mAbs. In the case of the M82G2 Fab, structures of the free Fab (PDB entry 1rfd), cocaine-bound Fab (PDB entry 1q72) and benzoylecgonine-bound Fab (PDB entry 1qyg) have been deposited in the Protein Data Bank. Pozharski *et al.* (2005) extensively discussed the Fab–cocaine binding interactions of the M82G2 (PDB entry 1q72) and GNC92H2 (PDB entry 1i7z; Larsen *et al.*, 2001) antibodies in view of their similar binding affinities and noted diversity of ligand recognition.

The binding site is a surface groove in both the h2E2 and M82G2 Fabs, as opposed to a deep pocket in the case of the GNC92H2 Fab. Different cocaine binding modes are observed in these antibodies owing to the differences in the CDR loop structures and in the placement of the aromatic residues in their respective heavy and light chains, which play an important role in recognition. A simple comparison of the number of van der Waals contacts between the ligand and the Fab shows that the number is larger for the M82G2 and GNC92H2 Fab complexes (Table 3) compared with the h2E2 Fab–benzoylecgonine complex. No hydrogen bonds (distance between non-H atoms of ≤3.2 Å between the ligand and the Fab) were observed between cocaine and the Fab in the two previously published complexes, but two hydrogen bonds were present between benzoylecgonine and Fab in the case of the M82G2 Fab complex (PDB entry 1qyg). Water-mediated hydrogen bonds were observed between the Fab and ligands in all structures (Table 3). Detailed calculations are warranted in order to understand the basis of the difference in affinities observed between the previously reported Fab complexes and that of h2E2.

5. Conclusion

The benzoylecgonine moiety is bound to a surface groove and its recognition by the h2E2 mAb is driven by the aromatic side chains of the Fab surrounding and trapping the tropane ring system of the ligand, forming significant van der Waals interactions that probably contribute to the nanomolar affinity observed. The smaller metabolites of cocaine such as ecgonine methyl ester and ecgonine are probably discriminated against by the antibody owing to the smaller hydrophobic surface presented by these metabolites to the antibody. It is likely that cocaine will bind in the same position as benzoylecgonine but accompanied by minor rearrangements of the hypervariable segments that could result in interactions with the methyl ester group of cocaine. Future refinements of the current study will require crystallization under conditions that inhibit the non-enzymatic hydrolysis of ester groups for the generation of Fab–cocaine and Fab–cocaethylene complex crystals. In addition, computational studies of binding free energies using free-energy perturbation methods may lead to a clearer understanding of the ligand-dependent binding properties observed for this antibody.

6. Related literature

The following references are cited in the supporting information for this article: Fishwild *et al.* (1996).

Acknowledgements

The Structural Biology Center beamlines are supported by the US Department of Energy, Office of Biological and Environmental Research under contract DE-AC02-06CH11357. The authors declare the following conflict of interest: Drs Norman and Ball are named as inventors on issued patents on the matter and the use of the h2E2 anti-cocaine monoclonal antibody.

Funding information

This work is supported in part by NIH grant U01DA039550 (Principal Investigator Andrew B. Norman).

References

Adams, P. D., Afonine, P. V., Bunkóczi, G., Chen, V. B., Davis, I. W., Echols, N., Headd, J. J., Hung, L.-W., Kapral, G. J., Grosse-Kunstleve, R. W., McCoy, A. J., Moriarty, N. W., Oeffner, R., Read, R. J., Richardson, D. C., Richardson, J. S., Terwilliger, T. C. & Zwart, P. H. (2010). *Acta Cryst.* D**66**, 213–221.

Carrera, M. R., Ashley, J. A., Parsons, L. H., Wirsching, P., Koob, G. F. & Janda, K. D. (1995). *Nature (London)*, **378**, 727–730.

Carrera, M. R., Ashley, J. A., Wirsching, P., Koob, G. F. & Janda, K. D. (2001). *Proc. Natl Acad. Sci. USA*, **98**, 1988–1992.
Carrera, M. R., Ashley, J. A., Zhou, B., Wirsching, P., Koob, G. F. & Janda, K. D. (2000). *Proc. Natl Acad. Sci. USA*, **97**, 6202–6206.
Carrera, M. R., Trigo, J. M., Wirsching, P., Roberts, A. & Janda, K. D. (2005). *Pharmacol. Biochem. Behav.* **81**, 709–714.
Cerny, E. H. & Cerny, T. (2008). *Expert Opin. Investig. Drugs*, **17**, 691–696.
Cowtan, K. (2008). *Acta Cryst.* D**64**, 83–89.
Das Gupta, V. (1982). *Int. J. Pharm.* **10**, 249–257.
Donnelly, M. I., Zhou, M., Millard, C. S., Clancy, S., Stols, L., Eschenfeldt, W. H., Collart, F. R. & Joachimiak, A. (2006). *Protein Expr. Purif.* **47**, 446–454.
Emsley, P., Lohkamp, B., Scott, W. G. & Cowtan, K. (2010). *Acta Cryst.* D**66**, 486–501.
Fishwild, D. M., O'Donnell, S. L., Bengoechea, T., Hudson, D. V., Harding, F., Bernhard, S. L., Jones, D., Kay, R. M., Higgins, K. M., Schramm, S. R. & Lonberg, N. (1996). *Nature Biotechnol.* **14**, 845–851.
Fox, B. S., Kantak, K. M., Edwards, M. A., Black, K. M., Bollinger, B. K., Botka, A. J., French, T. L., Thompson, T. L., Schad, V. C., Greenstein, J. L., Gefter, M. L., Exley, M. A., Swain, P. A. & Briner, T. J. (1996). *Nature Med.* **2**, 1129–1132.
Kim, Y., Dementieva, I., Zhou, M., Wu, R., Lezondra, L., Quartey, P., Joachimiak, G., Korolev, O., Li, H. & Joachimiak, A. (2004). *J. Struct. Funct. Genomics*, **5**, 111–118.
Kirley, T. L. & Norman, A. B. (2015). *Hum. Vaccin. Immunother.* **11**, 458–467.
Koschubs, T., Dengl, S., Dürr, H., Kaluza, K., Georges, G., Hartl, C., Jennewein, S., Lanzendörfer, M., Auer, J., Stern, A., Huang, K.-S., Packman, K., Gubler, U., Kostrewa, D., Ries, S., Hansen, S., Kohnert, U., Cramer, P. & Mundigl, O. (2012). *Biochem. J.* **442**, 483–494.
Kosten, T. R. & Owens, S. M. (2005). *Pharmacol. Ther.* **108**, 76–85.
Kvello, A. M., Andersen, J. M., Oiestad, E. L., Morland, J. & Bogen, I. L. (2016). *J. Pharmacol. Exp. Ther.* **358**, 181–189.
Lape, M., Paula, S. & Ball, W. J. (2010). *Eur. J. Med. Chem.* **45**, 2291–2298.
Larsen, N. A., Zhou, B., Heine, A., Wirsching, P., Janda, K. D. & Wilson, I. A. (2001). *J. Mol. Biol.* **311**, 9–15.
Laskowski, R. A. & Swindells, M. B. (2011). *J. Chem. Inf. Model.* **51**, 2778–2786.
Martell, B. A., Mitchell, E., Poling, J., Gonsai, K. & Kosten, T. R. (2005). *Biol. Psychiatry*, **58**, 158–164.
Martell, B. A., Orson, F. M., Poling, J., Mitchell, E., Rossen, R. D., Gardner, T. & Kosten, T. R. (2009). *Arch. Gen. Psychiatry*, **66**, 1116–1123.
McCoy, A. J., Grosse-Kunstleve, R. W., Adams, P. D., Winn, M. D., Storoni, L. C. & Read, R. J. (2007). *J. Appl. Cryst.* **40**, 658–674.
Minor, W., Cymborowski, M., Otwinowski, Z. & Chruszcz, M. (2006). *Acta Cryst.* D**62**, 859–866.
Murray, J. B. & Al-Shora, H. I. (1978). *J. Clin. Pharm. Ther.* **3**, l–6.
Norman, A. B. & Ball, W. J. (2012). *Immunotherapy*, **4**, 335–343.
Norman, A. B., Gooden, F. C. T., Tabet, M. R. & Ball, W. J. (2014). *Drug Metab. Dispos.* **42**, 1125–1131.
Norman, A. B., Norman, M. K., Buesing, W. R., Tabet, M. R., Tsibulsky, V. L. & Ball, W. J. (2009). *J. Pharmacol. Exp. Ther.* **328**, 873–881.
Norman, A. B., Tabet, M. R., Norman, M. K., Buesing, W. R., Pesce, A. J. & Ball, W. J. (2007). *J. Pharmacol. Exp. Ther.* **320**, 145–153.
Paula, S., Tabet, M. R., Farr, C. D., Norman, A. B. & Ball, W. J. (2004). *J. Med. Chem.* **47**, 133–142.
Pozharski, E., Moulin, A., Hewagama, A., Shanafelt, A. B., Petsko, G. A. & Ringe, D. (2005). *J. Mol. Biol.* **349**, 570–582.
Rosenbaum, G., Alkire, R. W., Evans, G., Rotella, F. J., Lazarski, K., Zhang, R.-G., Ginell, S. L., Duke, N., Naday, I., Lazarz, J., Molitsky, M. J., Keefe, L., Gonczy, J., Rock, L., Sanishvili, R., Walsh, M. A., Westbrook, E. & Joachimiak, A. (2006). *J. Synchrotron Rad.* **13**, 30–45.
Schiweck, W. & Skerra, A. (1995). *Proteins*, **23**, 561–565.
Schlapschy, M., Grimm, S. & Skerra, A. (2006). *Protein Eng. Des. Sel.* **19**, 385–390.
Skerra, A. (1994*a*). *Gene*, **141**, 79–84.
Skerra, A. (1994*b*). *Gene*, **151**, 131–135.
Stanfield, R. L., Zemla, A., Wilson, I. A. & Rupp, B. (2006). *J. Mol. Biol.* **357**, 1566–1574.
Tan, K., Kim, Y., Hatzos-Skintges, C., Chang, C., Cuff, M., Chhor, G., Osipiuk, J., Michalska, K., Nocek, B., An, H., Babnigg, G., Bigelow, L., Joachimiak, G., Li, H., Mack, J., Makowska-Grzyska, M., Maltseva, N., Mulligan, R., Tesar, C., Zhou, M. & Joachimiak, A. (2014). *Methods Mol. Biol.* **1140**, 189–200.
Treweek, J. B. & Janda, K. D. (2012). *Mol. Pharm.* **9**, 969–978.
Vagin, A. & Teplyakov, A. (2010). *Acta Cryst.* D**66**, 22–25.
Walter, T. S., Meier, C., Assenberg, R., Au, K. F., Ren, J., Verma, A., Nettleship, J. E., Owens, R. J., Stuart, D. I. & Grimes, J. M. (2006). *Structure*, **14**, 1617–1622.
Warner, A. & Norman, A. B. (2000). *Ther. Drug Monit.* **22**, 266–270.
Wetzel, H. N., Tsibulsky, V. L. & Norman, A. B. (2016). *Drug Alcohol Depend.* **168**, 287–292.
Yanisch-Perron, C., Vieira, J. & Messing, J. (1985). *Gene*, **33**, 103–119.
Zhu, X., Dickerson, T. J., Rogers, C. J., Kaufmann, G. F., Mee, J. M., McKenzie, K. M., Janda, K. D. & Wilson, I. A. (2006). *Structure*, **14**, 205–216.